Study of Natural Convection in a Triangular Cavity Filled with Water: Application of the Lattice Boltzmann Method

Imen Mejri, Ahmed Mahmoudi, Mohamed A. Abbassi, Ahmed Omri

Abstract—The Lattice Boltzmann Method (LBM) with double populations is applied to solve the steady-state laminar natural convective heat transfer in a triangular cavity filled with water. The bottom wall is heated, the vertical wall is cooled, and the inclined wall is kept adiabatic. The buoyancy effect was modeled by applying the Boussinesq approximation to the momentum equation. The fluid velocity is determined by D2Q9 LBM and the energy equation is discritized by D2Q4 LBM to compute the temperature field. Comparisons with previously published work are performed and found to be in excellent agreement. Numerical results are obtained for a wide range of parameters: the Rayleigh number from 10^3 to 10^6 and the inclination angle from 0° to 360°. Flow and thermal fields were exhibited by means of streamlines and isotherms. It is observed that inclination angle can be used as a relevant parameter to control heat transfer in right-angled triangular enclosures.

Keywords—Heat transfer, inclination angle, Lattice Boltzmann Method, Nusselt number, Natural convection, Rayleigh number.

I. INTRODUCTION

THE Lattice Boltzmann Method (LBM) is emerged as a powerful tool to simulate fluid flow, heat and mass transfer. It has become a novel alternative to conventional Computational Fluid Dynamics (CFD) solvers like Finite Difference Method (FDM), Finite Element Method (FEM) and Finite Volume Method (FVM) for solving the Navier–Stokes Equations (NSE) [1]. The advantages of LBM include simple calculation procedures and easy-implementation boundary conditions. It is well suitable for parallel computation, ease and robust in handling of multiphase flow and can be applied for complex geometries. Moreover when using LBM the coupling between pressure and velocity field is avoided; in conventional classical methods this linkage is handled by algorithms such as SIMPLE, SIMPLER [2] and others which are CPU time consumers. Another advantage it is that can capture turbulence without any turbulence models [3]. More details about the LBM can be found in the reference [4]-[6]. Standard benchmark problems have been simulated by LBM and the results were shown to agree well with the classical CFD solvers [7]. Many works dealing with convection in enclosures are restricted to the cases of simple geometry,

rectangular, cylindrical or spherical cavities. But the real configurations are complex and varied. Natural convection in triangular enclosures has received increased attention due to its direct relevancy to many engineering applications because of its applications to real life configurations such as thermal insulation of buildings using air gaps, solar energy collectors, furnaces and fire control in buildings. A few studies on natural convection on triangular enclosures filled with a viscous fluid have been carried out by earlier researchers [8]-[11]. Asan and Namli [12] presented a computational study of natural convection in an isosceles triangular enclosure with a hot horizontal base and cold inclined walls. They used the stream function-vorticity formulation in conjunction with the volume control integration solution technique. Steady state solutions were obtained for Rayleigh number ranging from 10^3 to 10^6. They showed that the height-base ratio and Rayleigh number have profound effect on temperature and flow field. Rahman et al. [13] investigated numerically the behavior of nanofluids in an inclined lid-driven triangular enclosure to gain insight into convective recirculation and flow processes induced by nanofluids. It is observed that solid volume fraction strongly influenced the fluid flow and heat transfer in the enclosure. Moreover, the variation of the average Nusselt number and average fluid temperature in the cavity is linear with the solid volume fraction. Koca et al. [14] analyzed the effect of Prandtl number on natural convection heat transfer and fluid flow in triangular enclosures with localized heating. The governing equations of natural convection are formulated based on a stream function–vorticity approach and solved with the finite-difference method. Bottom wall of triangle is heated partially while inclined wall is maintained at a lower uniform temperature than heated wall while remaining walls are insulated. It is observed that both flow and temperature fields are affected with the changing of Prandtl number, location of heater and length of heater as well as Rayleigh number. Omri et al. [15] deal with a numerical simulation of natural convection flows in a triangular cavity submitted to a uniform heat flux using the Control Volume Finite Element Method (CVFEM). Their results showed that the flow structure is sensitive to the cover tilt angle. Many recirculation zones can occur in the core cavity and the heat transfer is dependent on the flow structure. Mahmoudi et al. [16] investigated numerically natural convection for a two-dimensional triangular enclosure with partially heated from below and cold inclined wall filled with nanofluid in presence of magnetic field. Governing equations are solved by finite volume

Imen Mejri is with Unité de Recherche Matériaux, Energie et Energies Renouvelables (MEER), Faculté des Sciences de Gafsa, B.P.19, Zarroug, Gafsa, 2112, Tunisie (Corresponding Author; e-mail : im.mejri85@yahoo.fr).

Ahmed Mahmoudi, Mohamed A. Abbassi, and Ahmed Omri are with Unité de Recherche Matériaux, Energie et Energies Renouvelables (MEER), Faculté des Sciences de Gafsa, B.P.19, Zarroug, Gafsa, 2112, Tunisie (e-mail: ahmed.mahmoudi@yahoo.fr, abbassima@gmail.com, ahom206@yahoo.fr).

method. Flow pattern, isotherms and average Nusselt number are presented for six studied cases that are made by location of heat sources. Their results show in presence of magnetic field flow field is suppressed and heat transfer decreases. Furthermore it is observed that maximum reduction of average Nusselt number in high value of Ha occurs at Ra = 10^6. They also found that the nanoparticles are more effective at Ra = 10^4 where conduction is more pronounced. Ghasemi and Aminossadati [17] presented a numerical study on the mixed convection in a lid-driven triangular enclosure filled with a water-Al_2O_3 nanofluid. A comparison study between two different scenarios of upward and downward left sliding walls is presented. The effects of parameters such as Richardson number, solid volume fraction and the direction of the sliding wall motion on the flow and temperature fields as well as the heat transfer rate are examined. The results show that the addition of Al_2O_3 nanoparticles enhances the heat transfer rate for all values of Richardson number and for each direction of the sliding wall motion. However, the downward sliding wall motion results in a stronger flow circulation within the enclosure and hence, a higher heat transfer rate. Varol [18] studied numerically heat transfer and fluid flow due to natural convection in a porous triangular enclosure with a centered conducting body. The center of the body was located onto the gravity center of the right-angle triangular cavity. The Darcy law model was used to write the governing equations and they were solved using a finite difference method. He concluded that both height and width of the body and thermal conductivity ratio play an important role on heat and fluid flow inside the cavity. Ching et al. [19] investigated numerically mixed convection heat and mass transfer in a right triangular enclosure is. The bottom surface of the enclosure is maintained at uniform temperature and concentration that are higher than that of the inclined surface. The study is performed for pertinent parameters such as. The effect of buoyancy ratio, Richardson number and the direction of the sliding wall motion parameters on the flow and temperature fields as well as the heat and mass transfer rate examined. The results show that the increase of buoyancy ratio enhances the heat and mass transfer rate for all values of Richardson number and for each direction of the sliding wall motion. However, the direction of the sliding wall motion can be a good control parameter for the flow and temperature fields.

Basak et al. [20] studied numerically entropy generation due to natural convection in right-angled triangular enclosures of various fluids (Pr = 0.025, 7, and 1000). The maximum value of entropy generation, due to fluid flow, is observed near middle portions of the side walls. The location of this maximum depends on the presence of high velocity gradients. Oztop et al. [21] studied experimentally and numerically, heat transfer in a right angle triangular isosceles cavity, filled with air. The bottom wall of the cavity is hot, the inclined wall is cold and the vertical wall is adiabatic. Numerical study is based on the finite difference method. Results, such as the average Nusselt number on the hot wall are shown experimentally and numerically for different angles and for two values of the Rayleigh number 1.5×10^4 and 1.5×10^5.

They showed, experimentally, the effect of Rayleigh number and inclination angle on natural convection in a triangular cavity. Gurkan et al. [22] studied experimentally and numerically natural convection in a triangular recess, isosceles and right, filled with water, the bottom wall is hot, the vertical wall is cold and the inclined wall is adiabatic. Numerical solutions are obtained using a CFD commercial software, FLUENT, using the finite volume method. They showed, experimentally, the effect of Rayleigh number on natural convection in a triangular cavity.

The aim of this paper is to study fluid flow and temperature distribution and to analyze the heat flow due to natural convection in a right angled triangular enclosure filled with water. The results are represented in terms of isotherms, streamlines, maximum of absolute value of the stream function, and average Nusselt number calculate on the hot wall. The LBM has been used to solve the non-linear coupled partial differential equations of flow and temperature fields.

II. MATHEMATICAL FORMULATION

A. Problem Statement

The cavity has the shape of an isosceles right-angled triangle. The cavity is heated from a wall, and cooled from the other wall. The third wall is adiabatic. The geometry of the present problem is shown in Fig. 1. The walls of the cavity are rigid. Mechanical and thermal boundary conditions are defined as follows:

Inclined wall: $\frac{\partial T}{\partial n} = 0$, $u = v = 0$

Vertical wall: $T(x = 0, 0 \le y \le H) = T_c$, $u = v = 0$

Bottom wall: $T(0 \le x \le L, y = 0) = T_h$, $u = v = 0$

B. Lattice Boltzmann Method

For the incompressible non isothermal problems, Lattice Boltzmann Method (LBM) utilizes two distribution functions, f and g, for the flow and temperature fields respectively.

For the flow field:

$$f_i(\mathbf{x} + \mathbf{c_i}\Delta t, t + \Delta t) = f_i(\mathbf{x}, t) - \frac{1}{\tau_v}\left(f_i(\mathbf{x}, t) - f_i^{eq}(\mathbf{x}, t)\right) + \Delta t F_i \quad (1)$$

For the temperature field:

$$g_i(\mathbf{x} + \mathbf{c_i}\Delta t, t + \Delta t) = g_i(\mathbf{x}, t) - \frac{1}{\tau_\alpha}\left(g_i(\mathbf{x}, t) - g_i^{eq}(\mathbf{x}, t)\right) \quad (2)$$

where the discrete particle velocity vectors defined by $\mathbf{c_i}$ (Fig. 2 (a) for the flow and (b) for the temperature), Δt denotes lattice time step which is set to unity. τ_v, τ_α are the relaxation time for the flow and temperature fields, respectively. f_i^{eq}, g_i^{eq} are the local equilibrium distribution functions that have an appropriately prescribed functional dependence on the local hydrodynamic properties which are calculated with (3) and (4) for flow and temperature fields respectively.

$$f_i^{eq} = w_i \rho \left[1 + \frac{3(\mathbf{c_i}.\mathbf{u})}{c^2} + \frac{9(\mathbf{c_i}.\mathbf{u})^2}{2c^4} - \frac{3\mathbf{u}^2}{2c^2} \right] \qquad (3)$$

$$g_i^{eq} = w_i' T \left[1 + 3\frac{\mathbf{c_i}.\mathbf{u}}{c^2} \right] \qquad (4)$$

$\mathbf{u}$ and ρ are the macroscopic velocity and density, respectively. c is the lattice speed which is equal to $\Delta x / \Delta t$ where Δx is the lattice space similar to the lattice time step Δt which is equal to unity, w_i is the weighting factor for flow, w_i' is the weighting factor for temperature. D2Q9 model for flow and D2Q4 model for temperature are used in this work so that the weighting factors and the discrete particle velocity vectors are different for these two models and they are calculated with (5)-(7) as follows:

For D2Q9

$$w_0 = \frac{4}{9}, w_i = \frac{1}{9} \text{ for } i = 1,2,3,4 \text{ and } w_i = \frac{1}{36} \text{ for } i = 5,6,7,8 \qquad (5)$$

$$\mathbf{c_i} = \begin{vmatrix} 0 & i = 0 \\ \begin{cases} c(\cos[(i-1)\pi/2]) \\ c(\sin[(i-1)\pi/2]) \end{cases} & i = 1,2,3,4 \\ \begin{cases} \sqrt{2}c(\cos[(i-5)\pi/2+\pi/4]) \\ \sqrt{2}c(\sin[(i-5)\pi/2+\pi/4]) \end{cases} & i = 5,6,7,8 \end{vmatrix} \qquad (6)$$

For D2Q4

The temperature weighting factor for each direction is equal to $w_i' = 1/4$.

$$\mathbf{c_i} = (\cos[(i-1)\pi/2], \sin[(i-1)\pi/2])c \qquad (7)$$
$$i = 1,2,3,4$$

The kinematic viscosity v and the thermal diffusivity α are then related to the relaxation time by (8):

$$v = \left[\tau_v - \frac{1}{2} \right] c_s^2 \Delta t \qquad \alpha = \left[\tau_\alpha - \frac{1}{2} \right] c_s^2 \Delta t \qquad (8)$$

where c_s is the lattice speed of sound witch is equals to $c_s = c / \sqrt{3}$. In the simulation of natural convection, the external force term F corresponding to the buoyancy force appearing in (1) is given by (9)

$$F_i = \frac{\mathbf{G}.(\mathbf{c_i} - \mathbf{u})}{c_s^2} f_i^{eq} \qquad (9)$$

with $\mathbf{G}$ is the external force acting per unit mass . In a natural convection problem it is calculated by the following equation:

$$\mathbf{G} = -\rho \beta \vec{g} (T - T_m) \qquad (10)$$

where $\vec{g}$ is the gravitational vector. With the Boussinesq approximation, all the fluid properties are constant except in the body force term where the fluid density varies as

$$\rho = \rho_m \left[1 - \beta(T - T_m) \right] \qquad (11)$$

where ρ_m is the density of the fluid at the mean temperature T_m and β is the thermal expansion coefficient.

The macroscopic quantities, $\mathbf{u}$ and T can be calculated by the mentioned variables, with (12)-(14).

$$\rho = \sum_i f_i \qquad (12)$$

$$\rho \mathbf{u} = \sum_i f_i \mathbf{c_i} \qquad (13)$$

$$T = \sum_i g_i \qquad (14)$$

C. Non Dimensional Parameters

By fixing Rayleigh number, Prandtl number and Mach number, the viscosity and thermal diffusivity are calculated from the definition of these non dimensional parameters.

$$v = m.Ma.c_s \sqrt{\frac{Pr}{Ra}} \qquad (15)$$

where m is number of lattices in y-direction. Rayleigh and Prandtl numbers are defined as

$$Ra = \frac{\beta g m^3 (T_h - T_c)}{v \alpha}$$

and

$$Pr = \frac{v}{\alpha},$$

respectively. Mach number should be less than $Ma = 0.3$ to insure an incompressible flow. Therefore, in the present study, Mach number was fixed at $Ma = 0.1$.

Nusselt number is one of the most important dimensionless parameters in the description of the convective heat transport. The local Nusselt number Nu_x and the average value Nu at the hot wall are calculated as:

$$Nu_x = -\frac{H}{T_h - T_c} \frac{\partial T}{\partial y}\bigg|_{y=0} \qquad (16)$$

$$Nu = \frac{1}{H} \int_0^H Nu_x dx \qquad (17)$$

D. Boundary Conditions

The implementation of boundary conditions is very important for the simulation. The distribution functions out of the domain are known from the streaming process. The unknown distribution functions are those toward the domain.

For Flow:

Bounce-back boundary conditions were applied on all solid boundaries, which mean that incoming boundary populations are equal to out-going populations after the collision.

For Temperature:

The bounce back boundary condition is used on the adiabatic wall. Temperature at the isothermal wall is known. Since we are using D2Q4, the unknown internal energy distribution functions are evaluated respectively as:

South wall: $\qquad g_2 = T_H - g_1 - g_3 - g_4 \qquad$ (18)

Vertical wall: $\qquad g_1 = T_C - g_2 - g_3 - g_4 \qquad$ (19)

III. CODE VALIDATION

The problem of convection in a triangular cavity has been studied by several authors, the validation of our code is tested first for a Rayleigh number equal to 2772 with the results obtained in [12], [23], and [24] by comparing the local Nuselt number (Fig. 3). The code is also tested with the experimental and numerical results obtained in [22] by comparing the streamlines and isothermal lines (Figs. 4 (a) and (b), 5 (a) and (b), 6 (a)-(c)), also by comparing the values of the stream functions for the range of Rayleigh number studied and for $\Phi = 0°$ (Table I), the relative error shows the good accuracy of the LBM.

In conclusion, the results of this code show good agreement with the published results. This shows that the present LBM code generates very accurate results compared with reference published results; moreover the LBM is a reliable tool for the solution of coupled flow and heat transfer.

IV. RESULTS AND DISCUSSION

In this section we will discuss the variation of the temperature distribution in the cavity by varying the Rayleigh number and by varying the inclination angle. For the Rayleigh number, it varies in the range of 10^3 to 10^6, while the inclination angle varies in the range of 0 ° to 360 °. The bold isotherm allows us to better monitor the variation of the temperature distribution; this line corresponds to the temperature

$$\frac{T - T_c}{T_h - T_c} = 0.5$$

$\Phi = 0°$ (Figs. 4 (a) and (b), 5 (a) and (b), and 6 (a)-(c)),When increasing the Rayleigh number convection is favored. For values of Rayleigh number above 10^5 convection is dominant. The maximum value of the stream function, for the Rayleigh number equal to 10^6, is 135 times as large as its value when the Rayleigh is equal to 10^3. Fluid flow within the cavity is more intense for the high values of Rayleigh; this causes the reduction of the thickness of boundary layer which is shown clearly in the isotherms.

$\Phi = 90°$ (Figs. 7 (a)-(e) and 8 (a)-(e)), the lower side is cold, the heat transfer is mainly by conduction even for large values of the Rayleigh number, this appears by the low values of the stream function and also by the distribution of temperature which is maintained unchanged for the upper value of the Rayleigh number. This means that the heat transfer does not controlled by convection. The fluid is stratified near the cold wall and the conduction is dominant.

$\Phi = 135°$ (Figs. 9 (a)-(e) and 10 (a)-(e)) Two contra-rotating cells are formed inside the cavity for all values of Rayleigh number, the top cell is rotating counterclockwise and the lower cell is rotating in the clockwise. The two cells are not symmetrical. The heat transfer is mainly by conduction even for large values of the Rayleigh number. The value of the stream function is low even for the large Rayleigh number values.

$\Phi = 225°$ (Figs. 11 (a)-(e) and 12 (a)-(e)), a single cell is formed rotating in the clockwise direction, the increase of Rayleigh number favors convection. For Rayleigh number values higher than 10^5 convection is dominant. This causes the reduction of the boundary layer.

$\Phi = 270°$ (Figs. 13 (a)-(e) and 14 (a)-(e)), the upper side is cold, the vertical side is hot, this implies that the heat transfer by convection is very intense for this angle. A single cell is formed by rotation in the clockwise direction. The more the value of the Rayleigh number increases, the more the convection is more dominant and the boundary layer becomes thinner.

$\Phi = 315°$ (Figs. 15 (a)-(e) and 16 (a)-(e)), the hot wall is at the bottom and the cold wall is at the top of the cavity. For the Rayleigh number equal to 10^3, the conduction is dominant. Two symmetric contra rotating cells are formed. The bottom cell is rotating in clockwise direction and the top cell is rotating in a counterclockwise direction. The temperature distribution inside the cavity is symmetrical. When increasing the Rayleigh number the convection regime is favored and the cells symmetry is broken.

Fig. 17 shows the variation of the maximum absolute value of the stream function by varying the inclination angle for the range of the Rayleigh number studied. Clearly $|\Psi|_{max}$ increases with the increase of the Rayleigh number, which means that the intensity of the flow increases with the increase of Rayleigh number. For Rayleigh number equal to 10^3, $|\Psi|_{max}$ is very low for all inclination angles, indicating that the heat transfer is mainly by conduction. For all values of the Rayleigh number, $|\Psi|_{max}$ admits a minimum value for $\Phi = 135°$, convection is not favored for this angle. The maximum values of $|\Psi|_{max}$ are obtained for $\Phi = 0°$ and 270°. For the values of the Rayleigh numbers equal to 5×10^5 and 10^6 the maximum value of the stream function is obtained for the angle 315°.

Fig. 18 shows the variation of the Nusselt number as function of the Rayleigh number for several inclination angles. Convection is dominant and the value of the Nusselt number

increases with increasing Rayleigh number. For the angles $\Phi = 90°$ and 135° conduction is dominant, and the Nusselt number is in its minimum value compared to the other angles. The highest values of the Nusselt number is obtained for $\Phi = 0°$, 270°, and 225° where convection is dominant. In addition to the Rayleigh number, it is clear that the inclination angle is a controlling parameter of heat transfer in the cavity.

V. CONCLUSION

In this work, it has been shown the ability of the Lattice Boltzmann Method with double population for the study of free convection in a triangular cavity filled with water. The range of the Rayleigh number is going from 10^3 to 10^6 and the inclination angle from 0° to 360°. The inclination angle and the Rayleigh number are two control parameters of the heat transfer.

(a)

(b)

Fig. 2 (a) Discrete velocity vectors for D2Q9, (b) Discrete velocity vectors for D2Q4

Fig. 1 Geometry of the present study

TABLE I

COMPARISON OF MAXIMUM ABSOLUTE VALUE OF THE STREAM FUNCTION WITH THE RESULTS OF LITERATURE

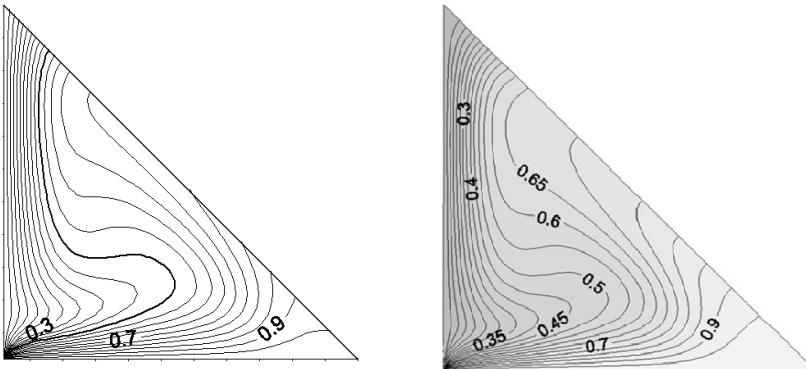| Ra	10^3	10^4	10^5	5×10^5	10^6
$|\psi|_{max}$ (LBM)	0.230	2.57	11.70	24.31	31.24
$|\psi|_{max}$ (reference)	0.215	2.62	12.12	25 .51	32.92
Error $(\%)$	6.97	1.90	3.46	4.70	5.10
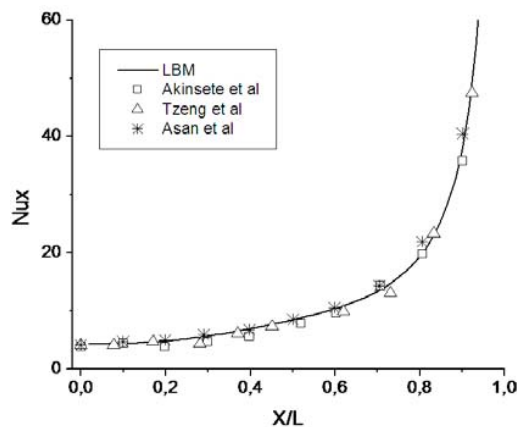
Fig. 3 Comparison of numerical results of local Nusselt numbers for triangular geometry with literature.
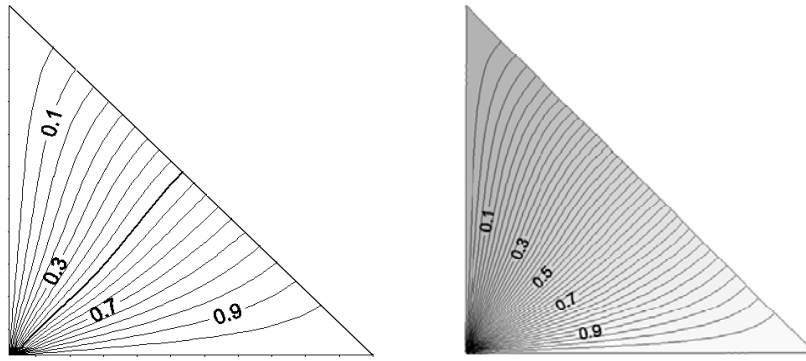
$Ra = 10^3$
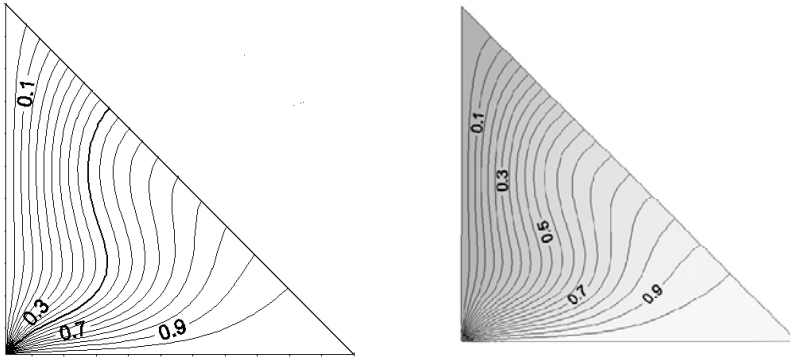
$Ra = 10^4$

$Ra = 10^5$
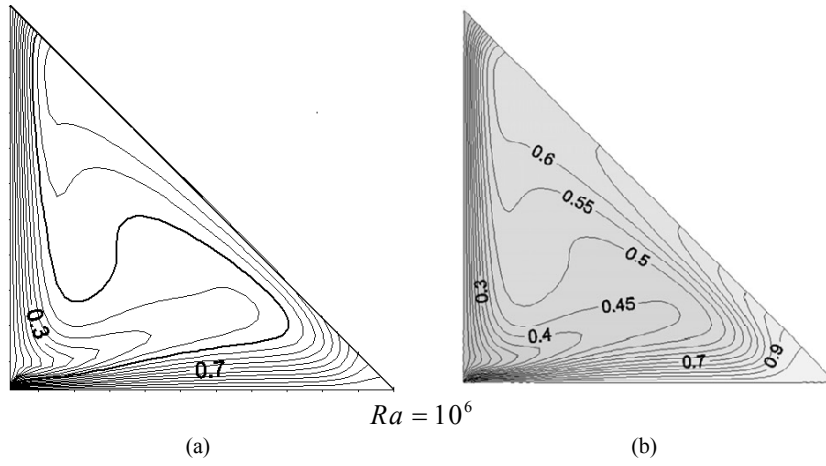
$Ra = 5 \times 10^5$

(a)   (b)

$$Ra = 10^6$$
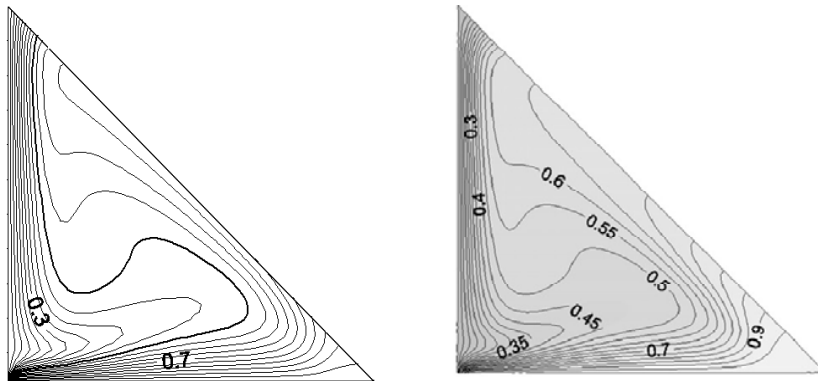
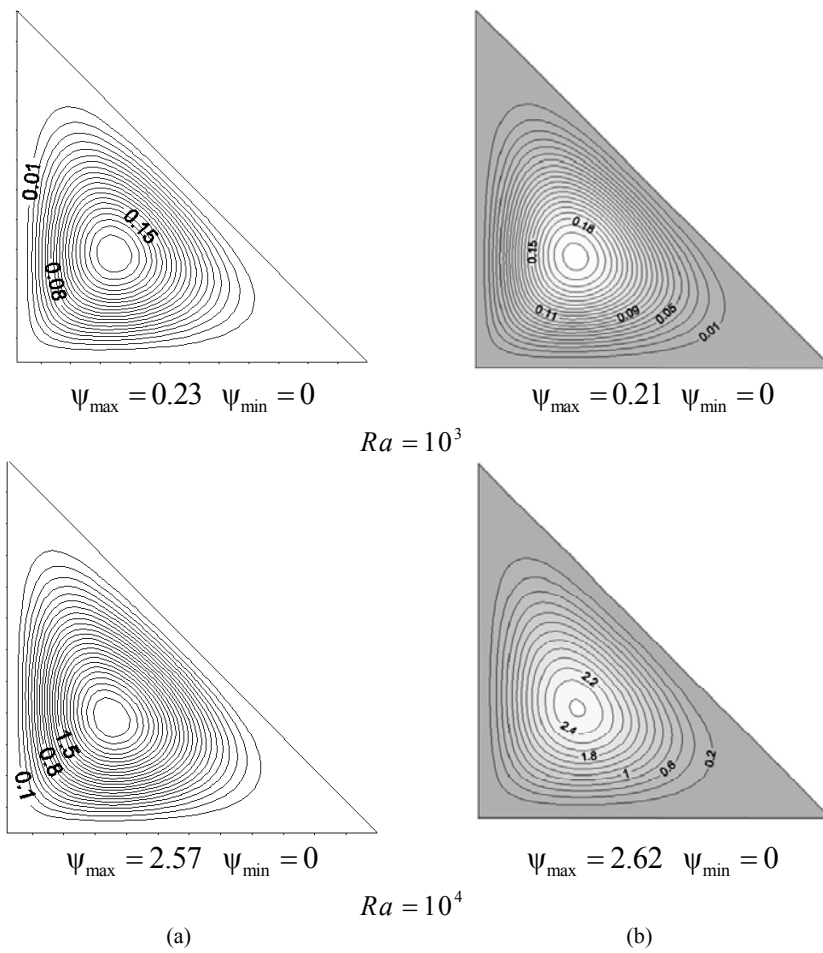(a)   (b)

Fig. 4 Isotherms (a) present study (b) Reference

$\psi_{max} = 0.23 \quad \psi_{min} = 0$ $\psi_{max} = 0.21 \quad \psi_{min} = 0$

$$Ra = 10^3$$

$\psi_{max} = 2.57 \quad \psi_{min} = 0$ $\psi_{max} = 2.62 \quad \psi_{min} = 0$

$$Ra = 10^4$$

(a)   (b)

Fig. 5 Streamlines (a) present study (b) Reference

$$\psi_{max} = 11.70 \quad \psi_{min} = 0 \qquad\qquad\qquad\qquad \psi_{max} = 12.12 \quad \psi_{min} = 0$$

$$Ra = 10^5$$

$$\psi_{max} = 24.30 \quad \psi_{min} = 0 \qquad\qquad\qquad\qquad \psi_{max} = 25.51 \quad \psi_{min} = 0$$

$$Ra = 5 \times 10^5$$

$$\psi_{max} = 31.24 \quad \psi_{min} = 0 \qquad\qquad\qquad\qquad \psi_{max} = 32.92 \quad \psi_{min} = 0$$

$$Ra = 10^6$$

(a)   (b)   (c)
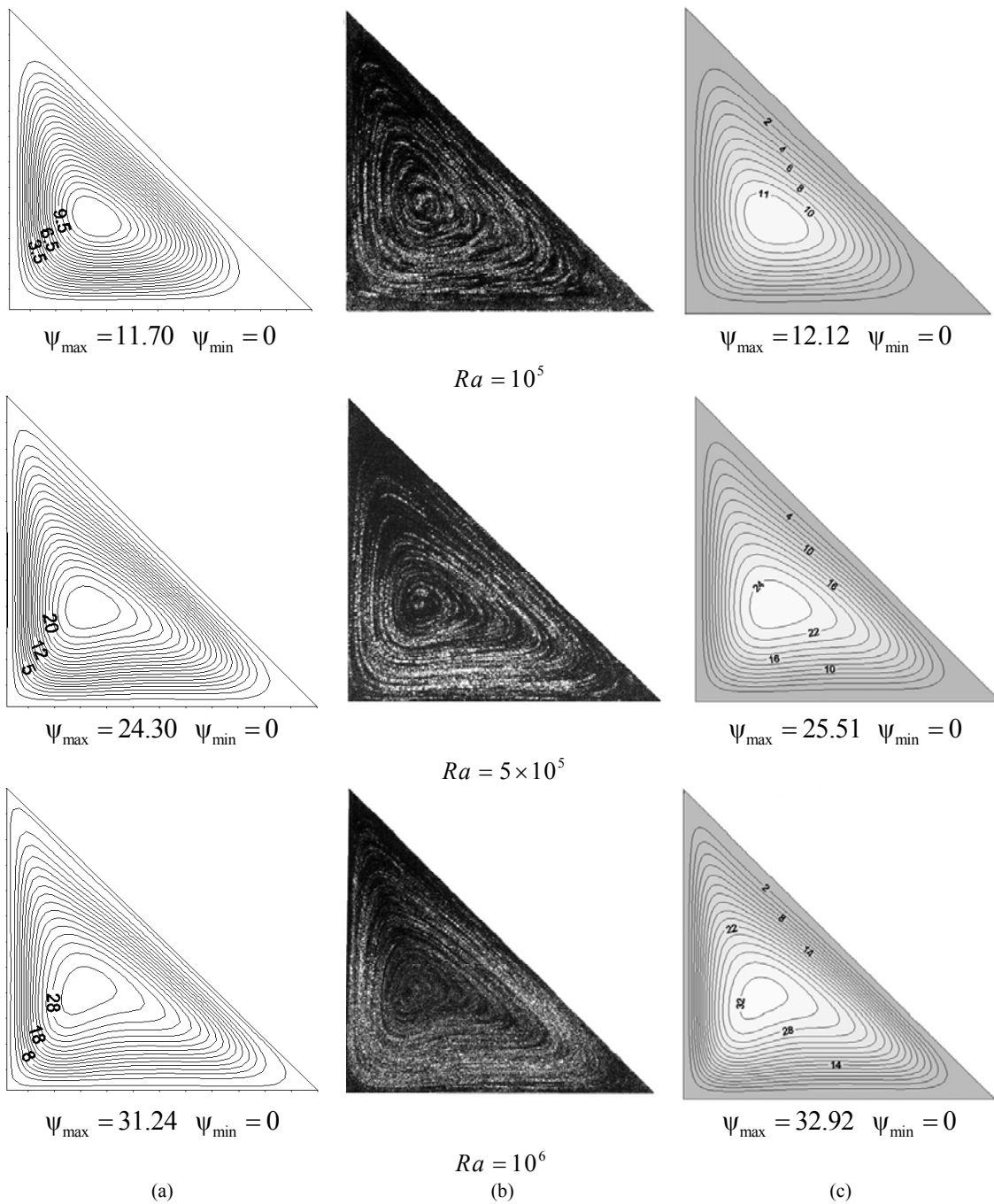
Fig. 6 Streamlines (a) present study, Reference: (b) experimental result and (c) numerical result

(a)　　　　　　　　　　　　(b)　　　　　　　　　　　　(c)

(d)　　　　　　　　　　　　　　　　　(e)

$$\Phi = 90°$$
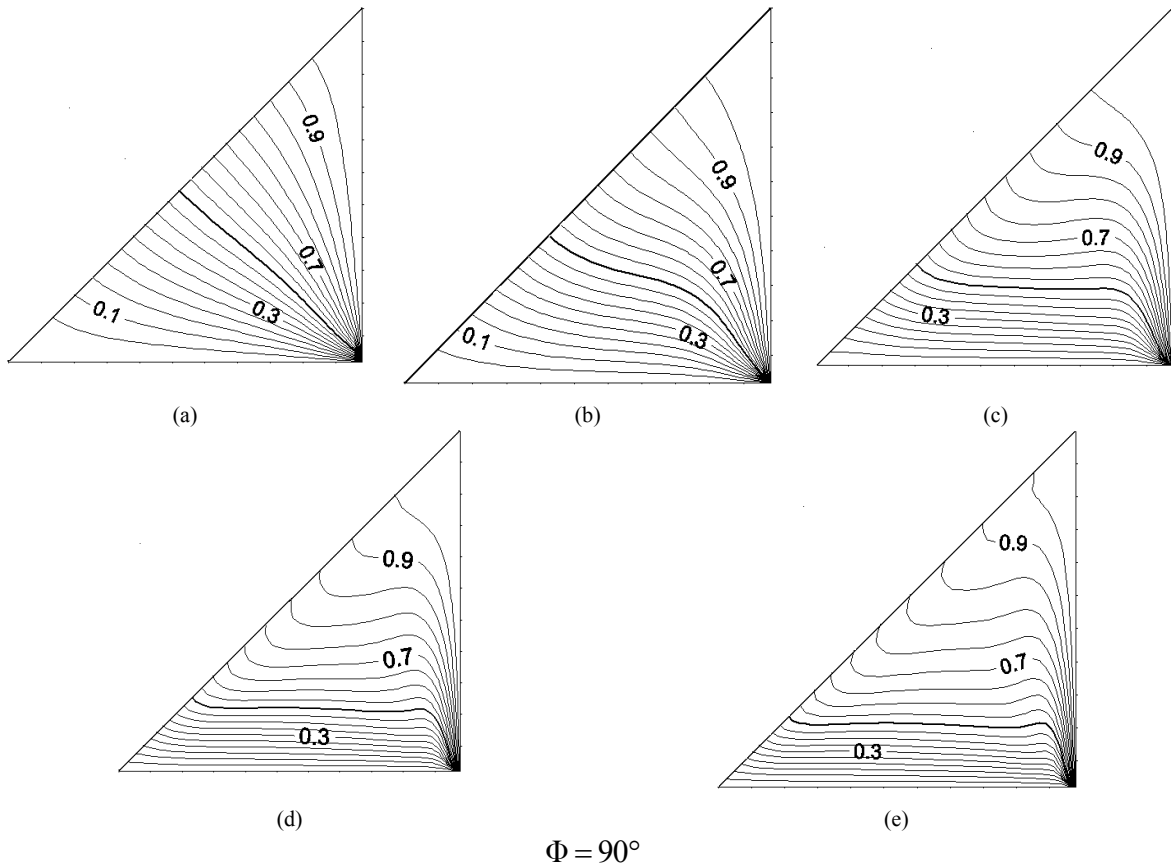
Fig. 7 Isotherms for $\Phi = 90°$ (a) $Ra = 10^3$, (b) 10^4, (c) 10^5, (d) 5×10^5 and (e) 10^6

$\psi_{max} = 0.21 \quad \psi_{min} = 0$　　$\psi_{max} = 1.26 \quad \psi_{min} = 0$　　$\psi_{max} = 3.69 \quad \psi_{min} = 0$

(a)　　　　　　　　　　　　(b)　　　　　　　　　　　　(c)

$$\psi_{max} = 6.11 \quad \psi_{min} = 0$$

(d)

$$\psi_{max} = 7.81 \quad \psi_{min} = 0$$

(e)

$$\Phi = 90°$$
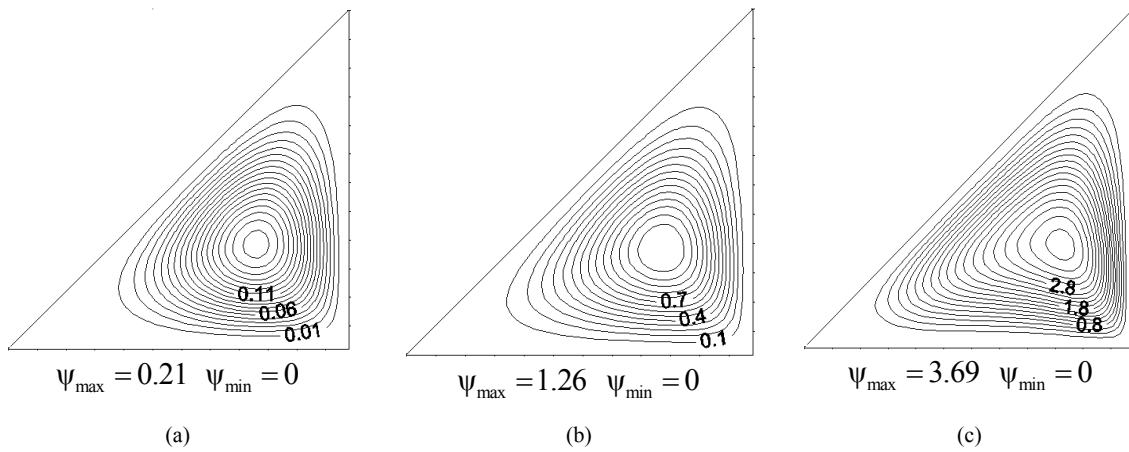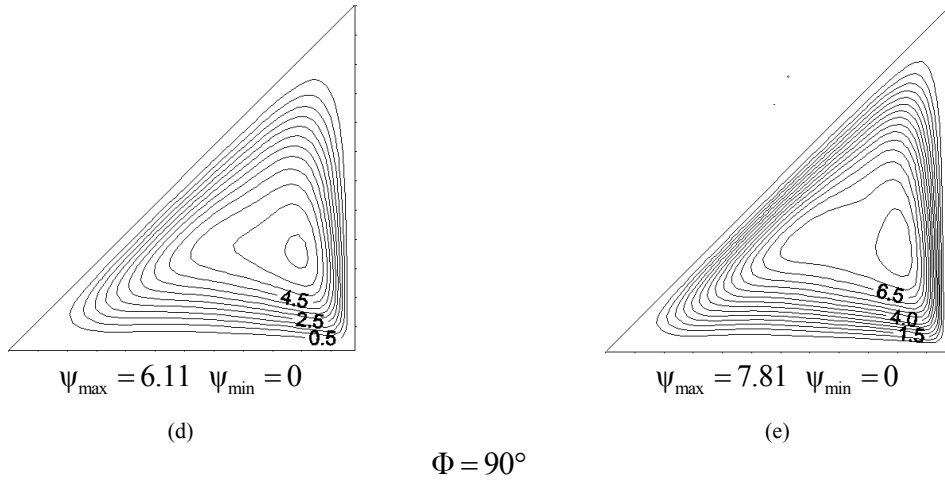
Fig. 8 Streamlines for $\Phi = 90°$ (a) $Ra = 10^3$, (b)10^4, (c)10^5, (d) 5×10^5 and (e) 10^6

(a)

(b)

(c)

(d)

(e)

$$\Phi = 135°$$
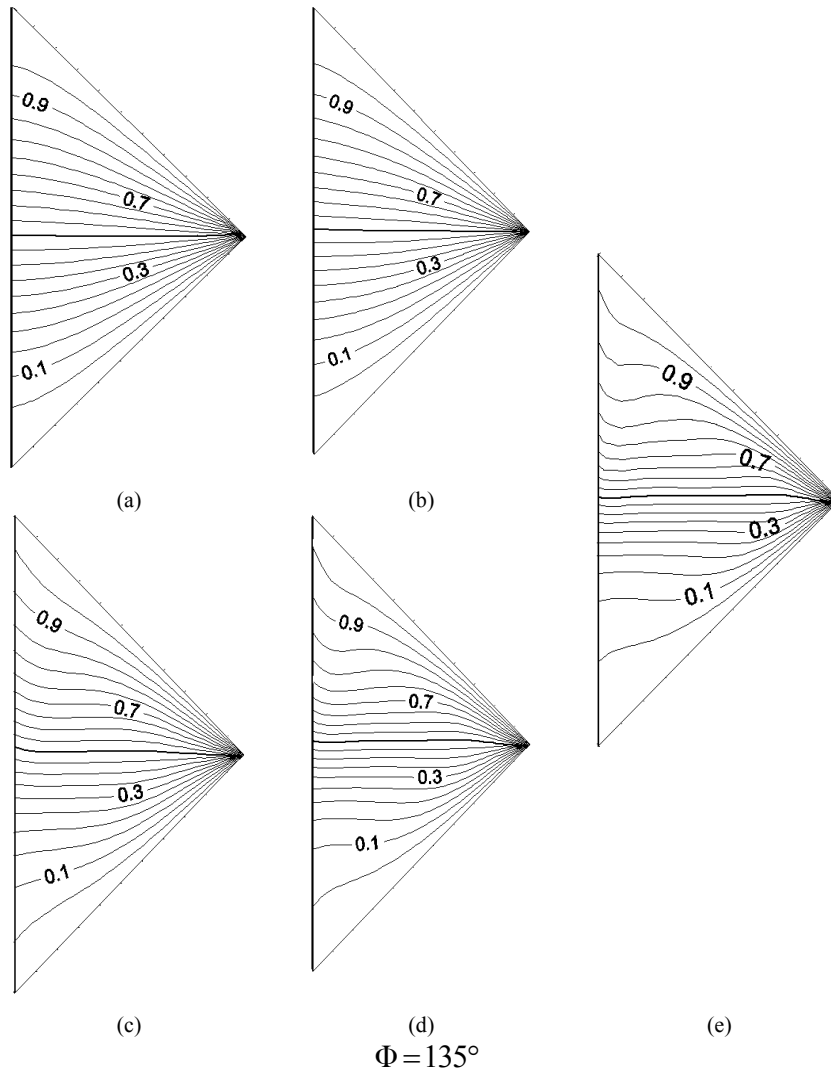
Fig. 9 Isotherms for $\Phi = 135°$ (a) $Ra = 10^3$, (b)10^4, (c)10^5, (d) 5×10^5 and (e) 10^6

$$\psi_{\max} = 0.037 \quad \psi_{\min} = -0.031$$

(a)

$$\psi_{\max} = 0.29 \quad \psi_{\min} = -0.18$$

(b)

$$\psi_{\max} = 5.71 \quad \psi_{\min} = -2.74$$

$$\psi_{\max} = 1.70 \quad \psi_{\min} = -1$$

(c)

$$\psi_{\max} = 3.91 \quad \psi_{\min} = -2.14$$

(d)

(e)

$$\Phi = 135°$$
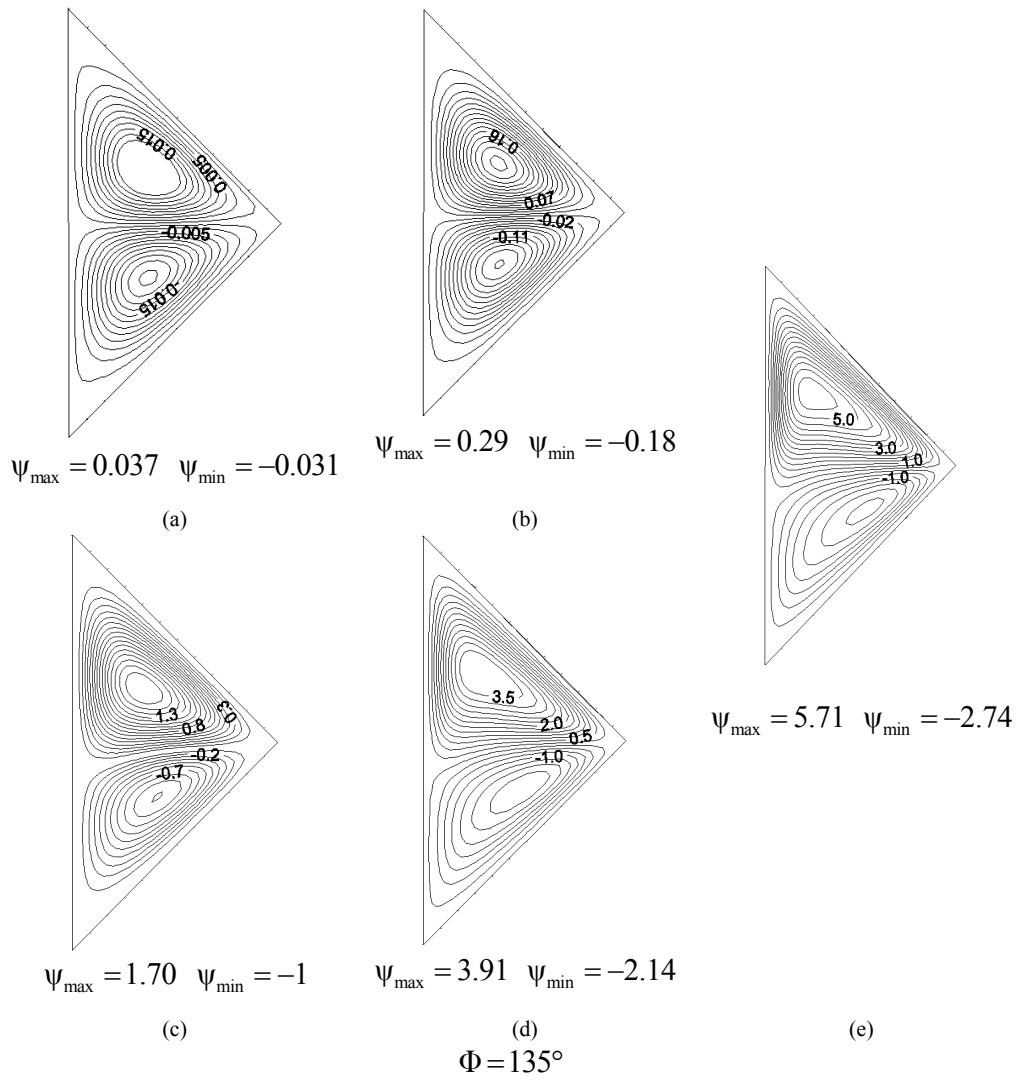
Fig. 10 Streamlines for $\Phi = 135°$ (a) $Ra = 10^3$, (b) 10^4, (c) 10^5, (d) 5×10^5 and (e) 10^6

(a)

(b)

(c)

(d)
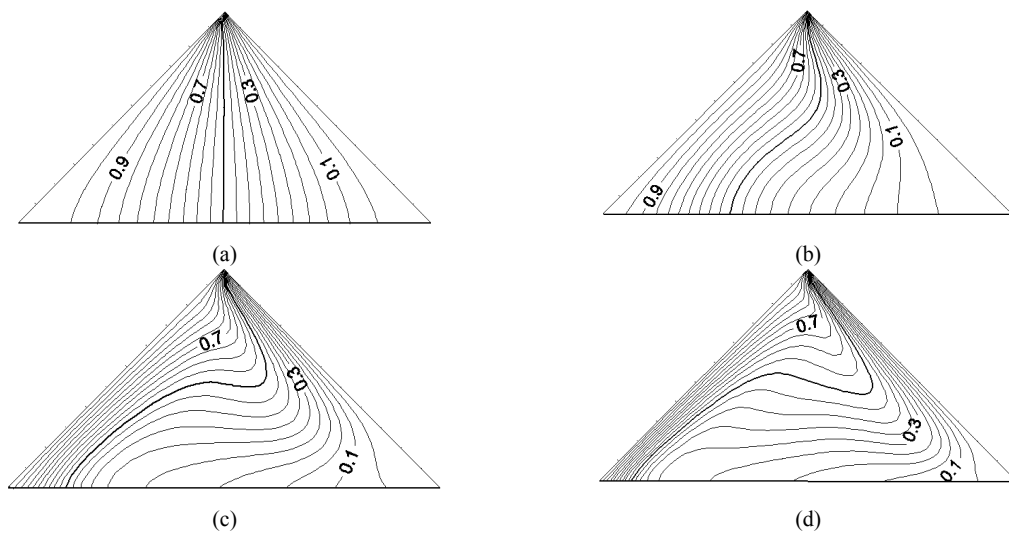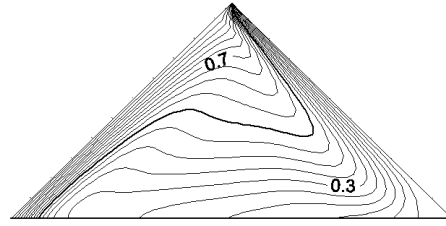
(e)

$$\Phi = 225°$$

Fig. 11 Isotherms for $\Phi = 225°$ (a) $Ra = 10^3$, (b) 10^4, (c) 10^5, (d) 5×10^5 and (e) 10^6
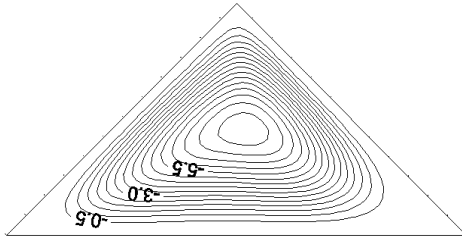
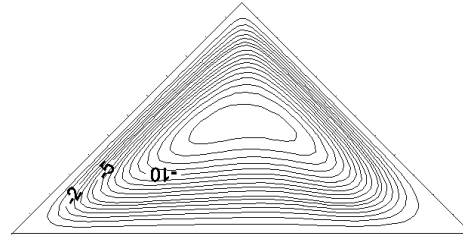

$\psi_{max} = 0 \quad \psi_{min} = -0.30$

(a)

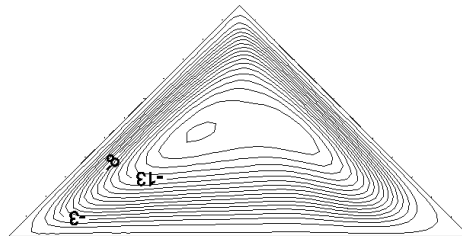$\psi_{max} = 0 \quad \psi_{min} = -2.20$

(b)

$\psi_{max} = 0 \quad \psi_{min} = -7.80$

(c)

$\psi_{max} = 0 \quad \psi_{min} = -13.68$

(d)
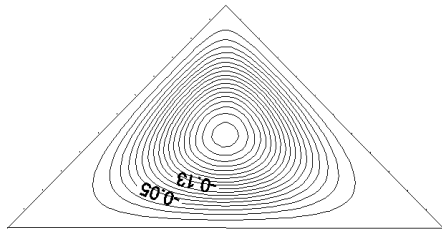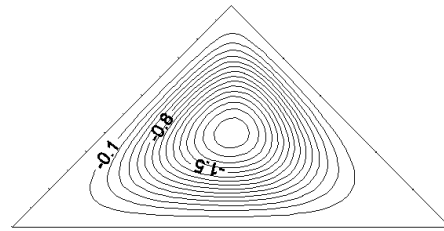
$\psi_{max} = 0 \quad \psi_{min} = -17.14$

(e)

$$\Phi = 225°$$

Fig. 12 Streamlines for $\Phi = 225°$ (a) $Ra = 10^3$, (b) 10^4, (c) 10^5, (d) 5×10^5 and (e) 10^6
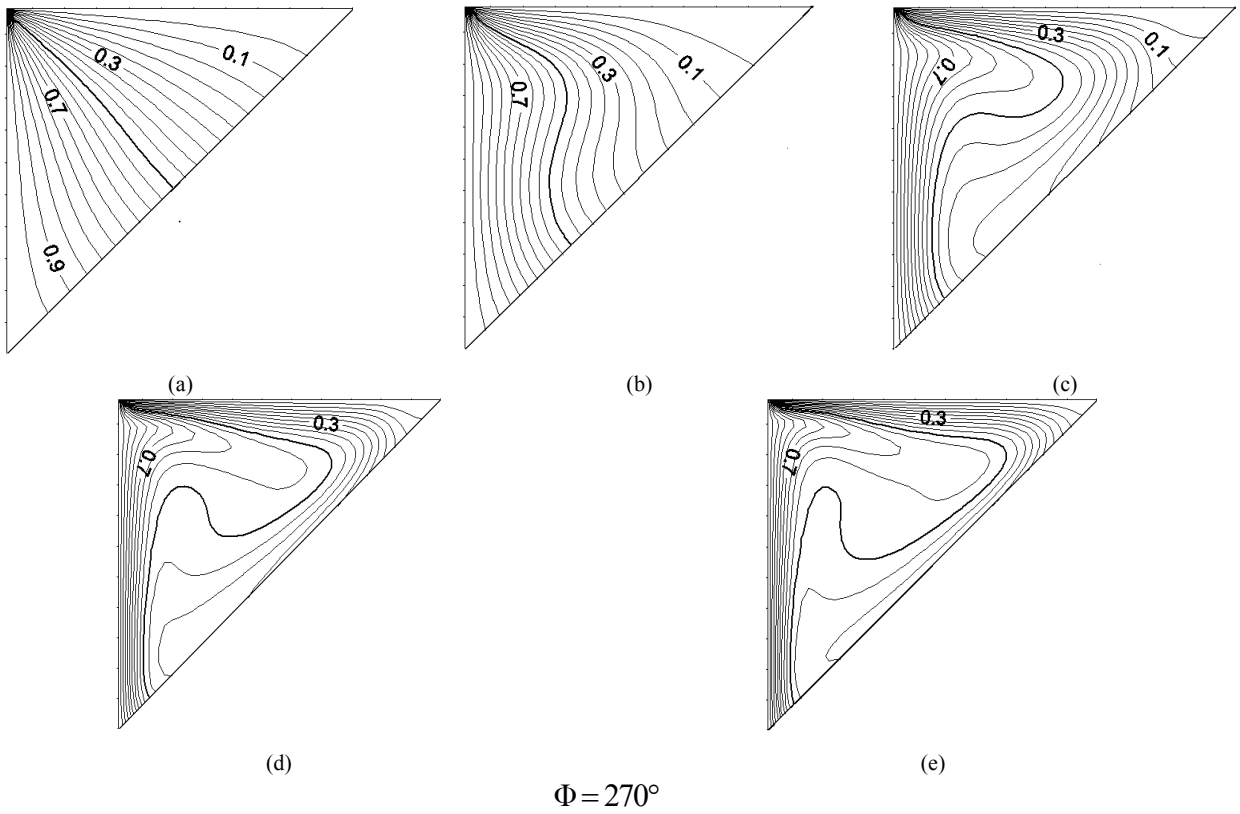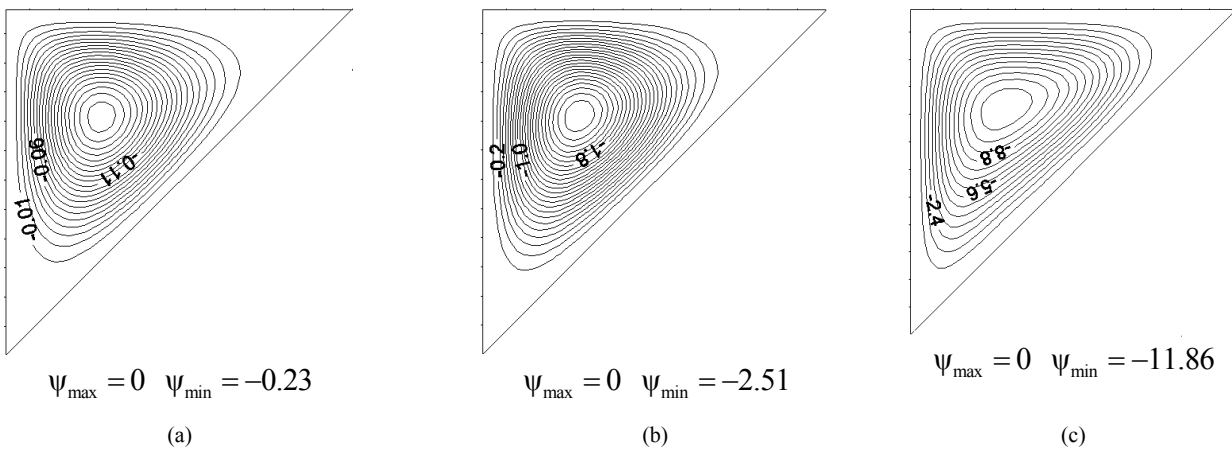
(a)   (b)   (c)

(d)   (e)

$$\Phi = 270°$$

Fig. 13 Isotherms for $\Phi = 270°$ (a) $Ra = 10^3$, (b) 10^4, (c) 10^5, (d) 5×10^5 and (e) 10^6

$$\psi_{max} = 0 \quad \psi_{min} = -0.23$$

(a)

$$\psi_{max} = 0 \quad \psi_{min} = -2.51$$

(b)

$$\psi_{max} = 0 \quad \psi_{min} = -11.86$$

(c)

$\psi_{max} = 0 \quad \psi_{min} = -25.14$

(d)

$\psi_{max} = 0 \quad \psi_{min} = -32.38$

(e)

$\Phi = 270°$
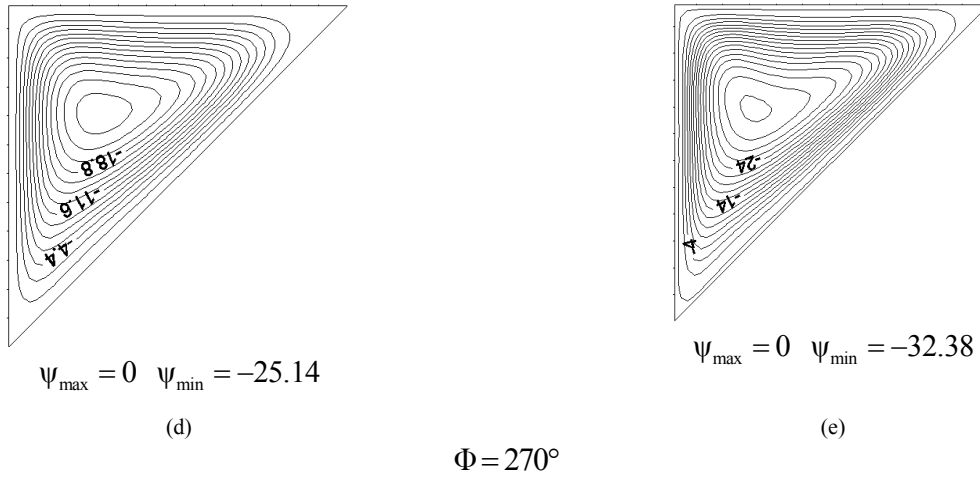
Fig. 14 Streamlines for $\Phi = 270°$ (a) $Ra = 10^3$, (b) 10^4, (c) 10^5, (d) 5×10^5 and (e) 10^6

(a)

(b)

(c)

(d)

(e)

$\Phi = 315°$
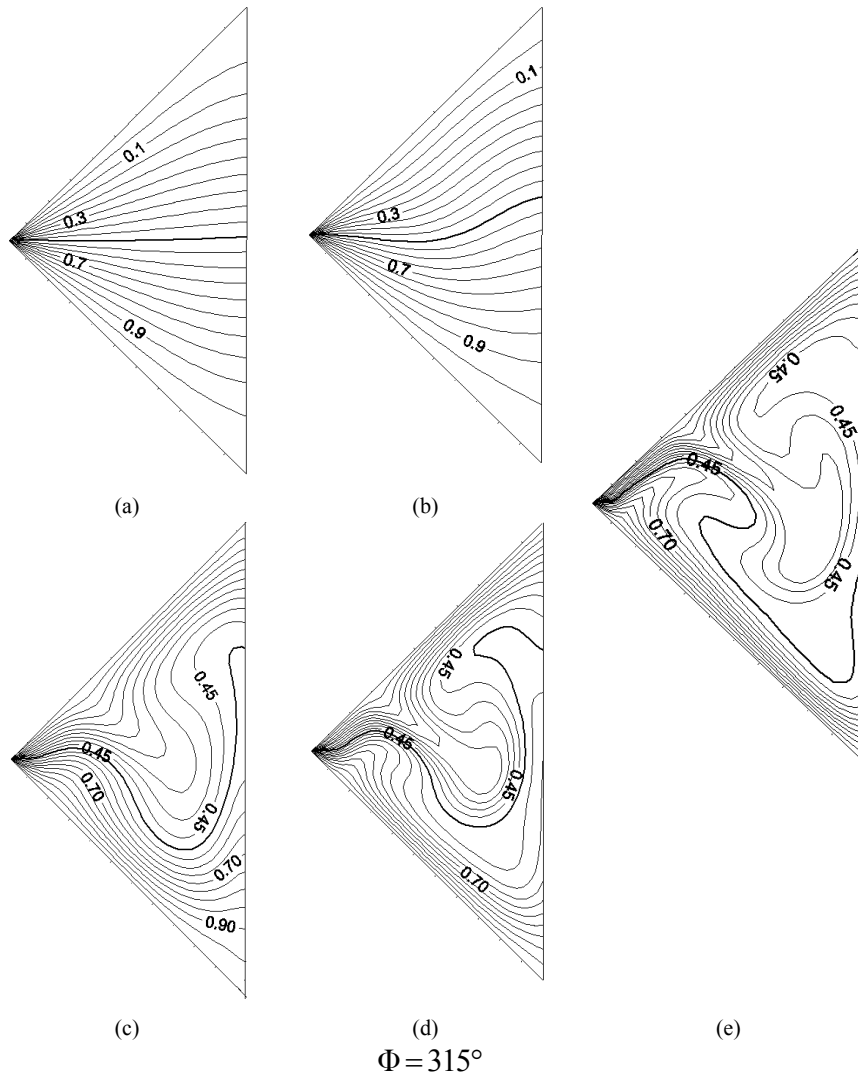
Fig. 15 Isotherms for $\Phi = 315°$ (a) $Ra = 10^3$, (b) 10^4, (c) 10^5, (d) 5×10^5 and (e) 10^6

$\psi_{\max} = 0.037 \quad \psi_{\min} = -0.030$

(a)

$\psi_{\max} = 0.78 \quad \psi_{\min} = -0.048$

(b)

$\psi_{\max} = 29.40 \quad \psi_{\min} = -35.17$

$\psi_{\max} = 6.30 \quad \psi_{\min} = -4.64$

(c)

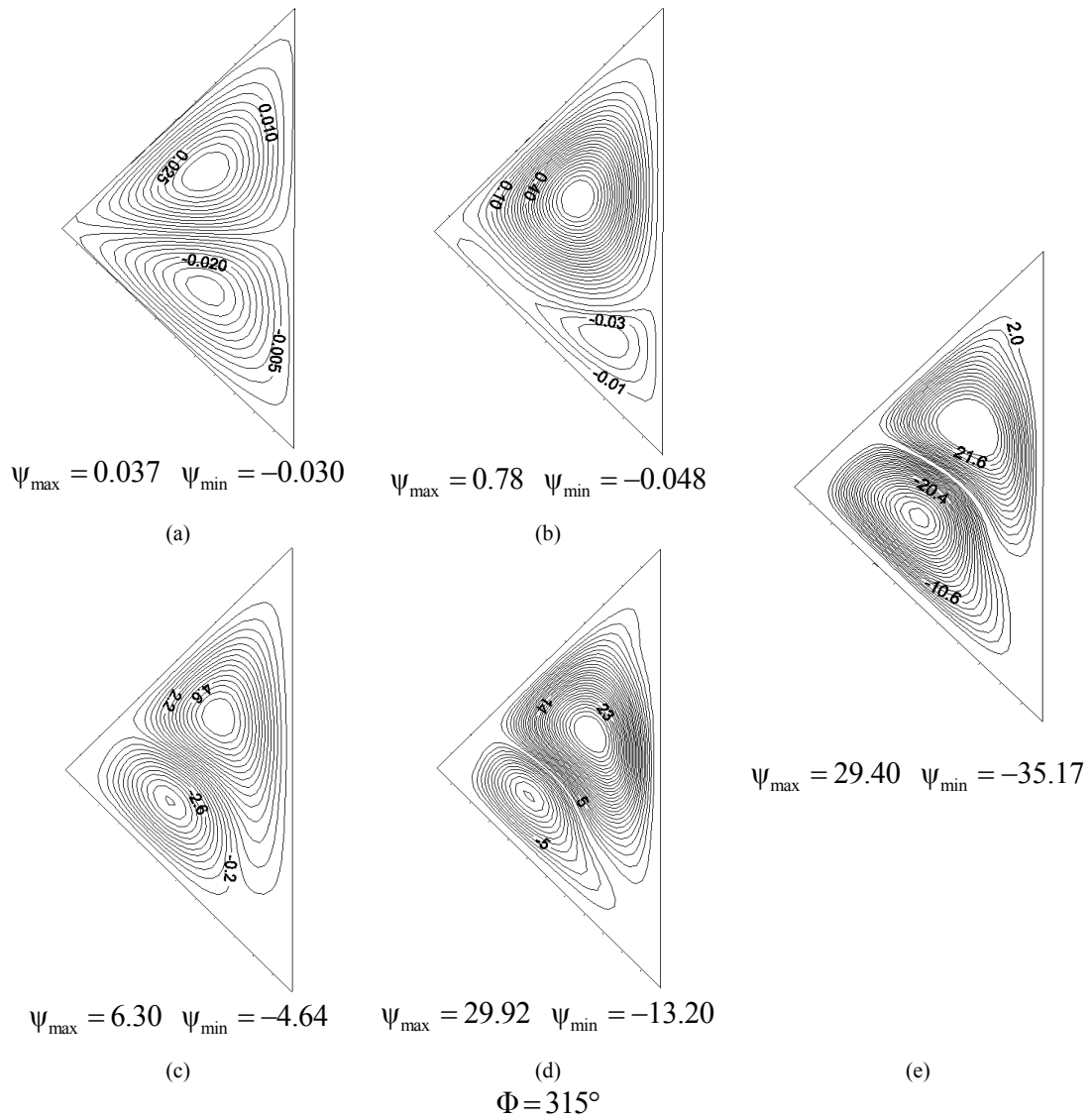$\psi_{\max} = 29.92 \quad \psi_{\min} = -13.20$

(d)

(e)

$\Phi = 315°$

Fig. 16 Streamlines for $\Phi = 315°$ (a) $Ra = 10^3$, (b) 10^4, (c) 10^5, (d) 5×10^5 and (e) 10^6
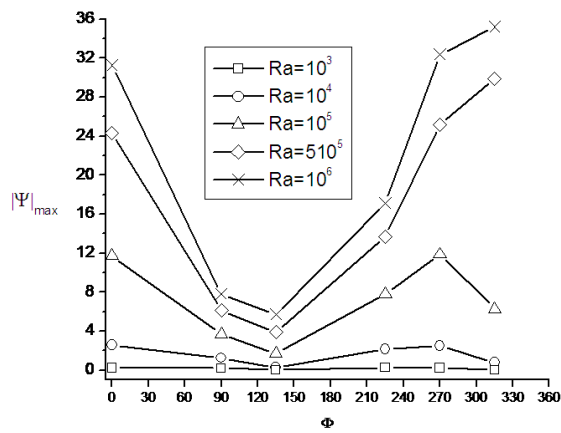
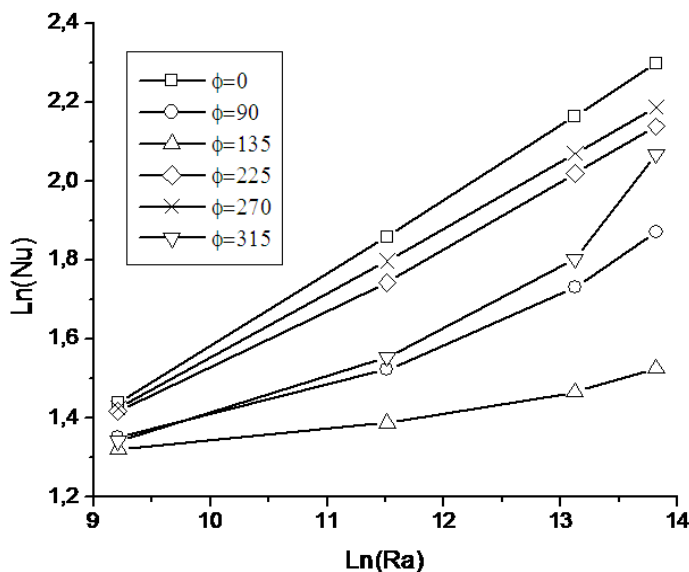Fig. 17 Variation of the maximum absolute value of the stream function by varying the inclination angle

Fig. 18 Average Nusselt number on the heated wall versus Rayleigh number

REFERENCES

[1] S. Chen and G.D. "Doolen, Lattice Boltzmann method for fluid flows", *Annual Review of Fluid Mechanics*, vol. 30, pp.329–64, 1998.

[2] S. V. Patankar, *Numerical Heat Transfer and Fluid Flow*, Hemisphere, Washington, D.C., 1980

[3] H. N. Dixit, V. Bab, "Simulation of high Rayleigh number natural convection in a square cavity using the lattice Boltzmann method". *Int.J. Heat Mass Transfer*, vol. 49, pp.727-39, 2006.

[4] F. J. Higuera, S. Succi, R. Benzi, "Lattice gas dynamics with enhanced collisions", *Europhys. Lett*. Vol. 9, pp. 345–349, 1989.

[5] R. Benzi, S. Succi, M. Vergassola, "The lattice Boltzmann equation: theory and applications", *Phys. Rep*. vol. 222, pp.145–197, 1992.

[6] S. Succi, *The Lattice Boltzmann Equation for Fluid Dynamics and Beyond*. Oxford University Press, 2001.

[7] G. McNamara and B. Alder. "Analysis of the lattice boltzmann treatment of hydrodynamic", *Physica A: Statistical Mechanics and its Applications*. Vol. 194, pp. 218–28, 1993.

[8] S. Ostrach, "Natural convection in enclosures", *J. Heat Transfer*. vol.110, pp. 1175–1190, 1988.

[9] I. Catton, "Natural convection in enclosures", *Proc. 6th Int. Heat Transfer Conf*. vol.6, pp. 13–31, 1978.

[10] B. Gebhart, Y. Jaluria, R.P. Mahajan, B. Sammakia, *Buoyancy-induced Flows and Transport*. Hemisphere, Washington, 1988.

[11] G. De Vahl Davis, "Natural convection of air in a square cavity: a bench mark numerical solution", *Int. J. Numer. Methods in Fluids*, vol. 3, pp. 249–264, 1983.

[12] H. Asan, L. Namli, "Numerical simulation of buoyant flow in a roof of triangular cross section under winter day boundary conditions", *Energy Buildings*, vol. 33, pp. 753-757, 2001.

[13] M.M. Rahman, M.M. Billah, A.T.M.M. Rahman, M.A. Kalam, A. Ahsan, "Numerical investigation of heat transfer enhancement of nanofluids in an inclined lid-driven triangular enclosure", *Int. Commun. Heat Mass Transfer*. vol. 38, pp. 1360–1367. 2011.

[14] A. Koca, H. F. Oztop, Y. Varol, "The effects of Prandtl number on natural convection in triangular enclosures with localized heating from below", *Int. Commun. Heat Mass Transfer*. vol. 34, pp. 511–519, 2007.

[15] A. Omri, "Numerical investigation on optimization of a solar distiller dimensions", *Desalination*, vol.206, pp. 373–379, 2007.

[16] A. H. Mahmoudi, I. Pop, M. Shahi,"Effect of magnetic field on natural convection in a triangular enclosure filled with nanofluid", *Int. J. Thermal Sciences*, vol. 59, pp. 126-140, 2012.

[17] B. Ghasemi, S.M. Aminossadati, "Mixed convection in a lid-driven triangular enclosure filled with nanofluids", *Int. Commun. Heat Mass Transfer*, vol. 37, pp. 1142-1148, 2010.

[18] Y. Varol, "Natural convection in porous triangular enclosure with a centered conducting body", *Int. Commun. Heat Mass Transfer*, vol. 38, pp. 368-376, 2011.

[19] Y. C. Ching , H. F. Oztop, M. M. Rahman, M. R. Islam, A. Ahsan, "Finite element simulation of mixed convection heat and mass transfer in a right triangular enclosure", *Int. Commun. Heat Mass Transfer*, vol.39, pp. 689-696, 2012.

[20] T. Basak, R. Anandalakshmi, P. Gunda, "Role of entropy generation during convective thermal processing in right-angled triangular enclosures with various wall heatings", *Chemical Engineering Research and Design*, vol. 90, pp.1779-1799, 2012.

[21] H. F. Oztop , Y. Varol , A. Koca, M. Firat , "Experimental and numerical analysis of buoyancy-induced flow in inclined triangular enclosures". *Int. Commun. Heat Mass Transfer*, vol. 39, pp.1237–1244, 2012.

[22] Y. Gurkan, A. Orhan, "Laminar natural convection in right-angled triangular enclosures heated and cooled on adjacent walls", *Int. J. Heat Mass Transfer*, vol. 60, pp. 365–374, 2013.

[23] S. C. Tzeng, J. H. Liou, R. Y . Jou, "Numerical simulation-aided parametric analysis of natural convection in a roof of triangular enclosures", *Heat Transfer Engineering*, vol. 26, pp. 69-79, 2005.

[24] V. Akinsete, T. A. Coleman, "Heat transfer by steady laminar free convection in triangular enclosures", *Int. J. Heat Mass Transfer*,vol. 25, pp. 991-998, 1982.